Bioorganic & Medicinal Chemistry Letters 18 (2008) 6071–6077

Contents lists available at ScienceDirect

Bioorganic & Medicinal Chemistry Letters

journal homepage: www.elsevier.com/locate/bmcl

Trifluoromethylpyrimidine-based inhibitors of proline-rich tyrosine kinase 2 (PYK2): Structure–activity relationships and strategies for the elimination of reactive metabolite formation

Daniel P. Walker *, F. Christopher Bi, Amit S. Kalgutkar, Jonathan N. Bauman, Sabrina X. Zhao, John R. Soglia, Gary E. Aspnes, Daniel W. Kung, Jacquelyn Klug-McLeod, Michael P. Zawistoski, Molly A. McGlynn, Robert Oliver, Matthew Dunn, Jian-Cheng Li, Daniel T. Richter, Beth A. Cooper, John C. Kath, Catherine A. Hulford, Christopher L. Autry, Michael J. Luzzio, Ethan J. Ung, W. Gregory Roberts, Peter C. Bonnette, Leonard Buckbinder, Anil Mistry, Matthew C. Griffor, Seungil Han, Angel Guzman-Perez

Pfizer Global Research and Development, Eastern Point Road, Groton, CT 06340, USA

ARTICLE INFO

Article history:
Received 7 September 2008
Revised 7 October 2008
Accepted 7 October 2008
Available online 11 October 2008

Keywords:
PYK2
FAK
Kinase
Osteoporosis
Bioactivation
Reactive metabolite

ABSTRACT

The synthesis and SAR for a series of diaminopyrimidines as PYK2 inhibitors are described. Using a combination of library and traditional medicinal chemistry techniques, a FAK-selective chemical series was transformed into compounds possessing good PYK2 potency and 10- to 20-fold selectivity against FAK. Subsequent studies found that the majority of the compounds were positive in a reactive metabolite assay, an indicator for potential toxicological liabilities. Based on the proposed mechanism for bioactivation, as well as a combination of structure-based drug design and traditional medicinal chemistry techniques, a follow-up series of PYK2 inhibitors was identified that maintained PYK2 potency, FAK selectivity and HLM stability, yet were negative in the RM assay.

© 2008 Elsevier Ltd. All rights reserved.

Proline-rich tyrosine kinase 2 (PYK2) and focal adhesion kinase (FAK) are nonreceptor tyrosine kinases, and together they constitute the FAK subfamily.[1] Unlike FAK expression, which is ubiquitous, PYK2 expression is relatively restricted, with highest levels in the brain and the hematopoietic system. In contrast to the embryonic lethality in FAK-deficient mice, PYK2 −/− mice are viable and fertile.[2] In a prior study, we found that the skeletal phenotype of adult PYK2 −/− female mice has significantly increased bone mass and bone mineral density compared to wild-type mice.[3] Furthermore, daily oral administration of a small-molecule PYK2 inhibitor (PF-431396, **1a**) resulted in an increase in bone formation and protection against bone loss in the ovariectomized (OVX) rat model, an established preclinical model of postmenopausal osteoporosis.[3] The fact that this efficacious response resulted from increased bone formation with minimal change in bone resorption has important therapeutic implications. Oral agents approved to treat osteoporosis include bisphosphonates, estrogen, and selective estrogen receptor modulators (SERMs), all of which are antiresorptive in nature and are insufficient for restoring bone in critically osteoporotic patients. Parathyroid hormone 1–34 is the only approved bone anabolic agent; however, it is an injectable that increases bone turnover with a balance favoring bone formation. Considering the usual challenges associated with protein-based therapeutics, such as inconvenient routes of administration, an orally bioavailable small-molecule PYK2 inhibitor represents an attractive anabolic therapy for patients afflicted by low bone mass and offers a new opportunity to impact this unmet medical need in the aging population.

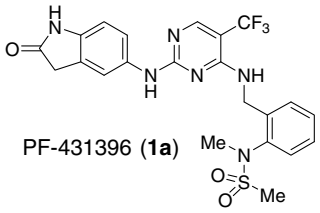

PF-431396 (**1a**)

Pyrimidine **1a** was an attractive compound due to its in vitro PYK2 potency (PYK2 IC_{50} = 31 nM) and in vivo efficacy.[3] However, subsequent studies accessing the bioactivation potential of **1a** and struc-

* Corresponding author. Tel.: +1 636 247 1192.
E-mail address: daniel.p.walker@pfizer.com (D.P. Walker).

0960-894X/$ - see front matter © 2008 Elsevier Ltd. All rights reserved.
doi:10.1016/j.bmcl.2008.10.030

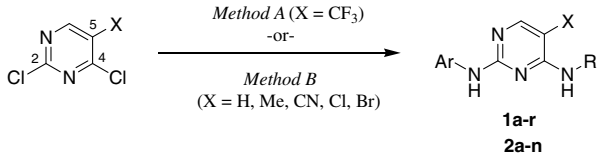

Scheme 1. General synthetic route for the preparation of pyrimidines of types **1** and **2**. *Method A* reagents and conditions: (a) 2.0 equiv, $ZnCl_2$ (1.0 M solution in ether), CH_2Cl_2–^tBuOH (1:1), −5 °C, 1 h; $ArNH_2$, 1.1 equiv Et_3N, −5 → 40 °C, 45–95%; (b) RNH_2, DMF, Na_2CO_3, 85 °C, 1–2 h, 60–95%. *Method B* reagents and conditions: (a) RNH_2, *i*-Pr_2NEt, THF, room temperature, 24 h, 75–95%; (b) $ArNH_2$, *i*-Pr_2NEt, dioxane, 110 °C, 24–48 h, 10–50%.

turally-related analogs in NADPH- and glutathione-ethyl ester (GSH-EE)-supplemented human liver microsomes (HLM) revealed the formation of sulfydryl conjugates, a phenomenon consistent with reactive metabolite formation. With an increasing awareness of potential toxicological liabilities that can occur via bioactivation of toxicophores within drug candidates,[4] we felt that it was important to identify the metabolic pathway responsible for reactive metabolite formation and to eliminate this undesirable attribute via rational structural modifications. We detail below the synthesis and structure–activity relationships (SARs) for a series of diamino pyrimidines as PYK2 inhibitors. We also detail our efforts to characterize the structure of the GSH conjugate of **1a**. This information provided insights into the structure of the reactive metabolite and the bioactivation pathway responsible for its formation thus allowing chemical intervention to eliminate the potential safety hurdle.

Pyrimidines of types **1** and **2** were prepared in two steps according to Scheme 1. Method A was utilized for pyrimidines possessing a trifluoromethyl group at C5,[5,6] whereas all other pyrimidines examined in this study were prepared by Method B.

Early in-house SAR studies on the pyrimidine series against the related kinase, FAK, identified 5-aminooxindole as a suitable C2 group (Table 1).[7] While other 6,5-fused heterocycles, such as indole **1b** and indazole **1c**, were also tolerated at this position, these heterocycles exhibited sub-optimal oral pharmacokinetics in the rat (oral bioavailability < 5%) due to a combination of poor aqueous solubility and first pass oxidative metabolism. SAR studies also identified trifluoromethyl as a suitable C5 group (compounds **1d–1i**). While the role of the C5 substituent in the inhibitory process is unclear, it is possible that the C5 substituent modulates the acidity of the C2 N–H bond, which is important for ligand binding to the kinase (vide infra). Further optimization of the pyrimidine series for PYK2 activity also found that 5-aminooxindole and trifluoromethyl were optimal C2 and C5 groups, respectively.

Not surprisingly, there was as well significant overlap in the SAR for PYK2 and FAK at the C4-position of the pyrimidine ring. This is likely due to the high degree of homology between PYK2 and FAK within the ATP binding pocket.[8] Nevertheless, some differences in the SARs were identified. For instance, whereas unsubstituted benzylamine **1j** showed a modest preference for FAK, *meta*-substitution significantly increased FAK activity and selectivity (compounds **1k** and **1l**). Conversely, *ortho*-substitution appeared to result in a modest selectivity for PYK2 (compounds **1m** and **1n**). *para*-Substitution resulted in decreased activity for both FAK and PYK2 (data not shown). In an effort to identify compounds with better HLM stability and PYK2 selectivity, we prepared a diversity library possessing aliphatic C4 amines. Two compounds emerged from these efforts, caprolactam **1o** and cyclopentanediamine **1p**, that showed good PYK2 potency and 6- to 10-fold selectivity against FAK. Cyclopentanediamine **1p** was further attractive in that it appeared to be stable in HLM towards oxidative metabolism.

During the course of the SAR studies to optimize PYK2 inhibitory potency and selectivity, it was observed that our early lead compound **1a** was positive in a high-throughput screen (HTS) for reactive metabolite formation. This screen examines the bioactivation potential of drug candidates in HLM via the detection of GSH and/or GSH-EE-captured reactive metabolites.[9] There are examples of drugs that are false positives in the HTS RM assay, yet are not associated with a significant incidence of toxicity.[10] However, since our interest was to develop a drug candidate for treating osteoporosis, which is a nonlife threatening disease, we felt it was important to eliminate the bioactivation liability within this chemical series. Liquid chromatography–tandem mass spectrometry (LC/MS/MS) analysis of the NADPH-supplemented HLM incubations containing **1a** and GSH or GSH-EE[9,11,12] led to the detection of sulfydryl conjugates with molecular ions (MH^+) at 812 (GSH) and 840 (GSH-EE), respectively. The formation of these conjugates was NADPH-dependent suggesting the involvement of cytochrome P450 in the bioactivation of **1a**. Also, inclusion of the specific P4503A4 inhibitor ketoconazole in the HLM incubations eliminated conjugate formation and overall metabolism implicating that P4503A4 was responsible for the oxidative metabolism/bioactivation of **1a**. Furthermore, in both cases, additional chromatographic separation revealed the presence of two isomeric peaks as depicted with the GSH conjugate of **1a** (Fig. 1, panel A). Overall, the molecular mass of the conjugate was consistent with the addition of one molecule of GSH or GSH-EE to the molecular mass of the parent compound **1a**.

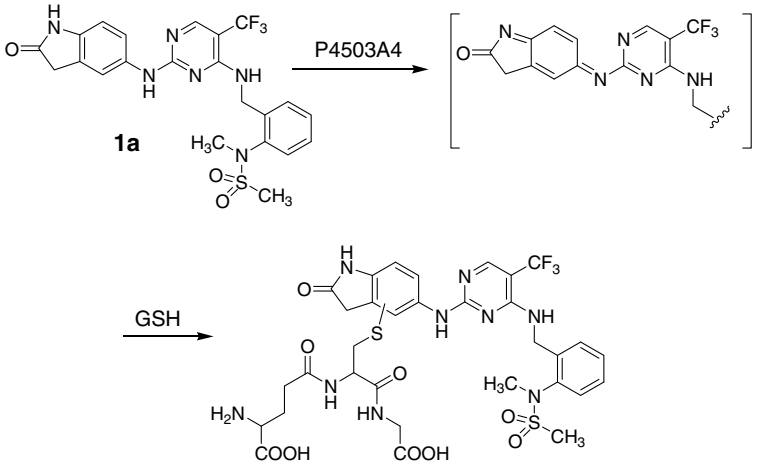

Scheme 2. Proposed mechanism of P450-catalyzed bioactivation of **1a**.

Table 1
In vitro IC_{50} values for FAK and PYK2 inhibition, HLM stability and propensity for reactive metabolite formation by compounds **1a–1r**

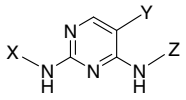

1a-r

Compound	X	Y	Z	FAK IC_{50}[a] (nM)	PYK2 IC_{50}[b] (nM)	HLM Eh[c]	RMA[d,e]
1a PF-431396	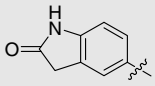	CF_3	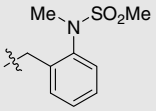	1.5 (n = 3)	11 (n = 3)[f]	0.78	Positive
1b	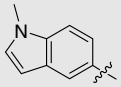	CF_3	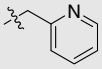	160	1200	>0.85	Positive
1c	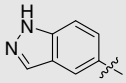	CF_3	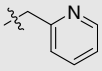	16	600	0.55	N.T.
1d	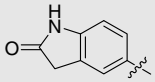	H	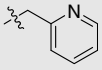	>10,000	>10,000	<0.26	Positive
1e	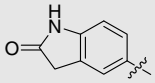	Me	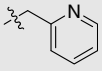	2200	>3000	<0.30	Positive
1f	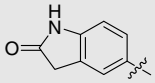	Cl	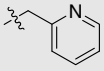	77 (n = 3)	>1000	<0.28	Positive
1g	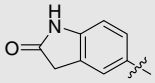	Br	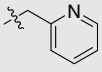	46 (n = 5)	580	0.44	N.T.
1h	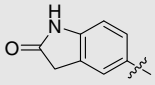	CN	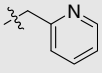	190	1800	<0.26	Positive
1i	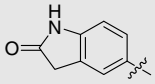	CF_3	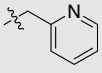	19	680	<0.26	Positive
1j	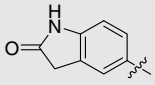	CF_3		34	120	<0.26	N.T.
1k	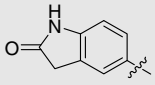	CF_3	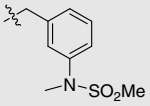	1.9 (n = 7)	190 (n = 7)	0.59	Positive
1l	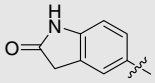	CF_3	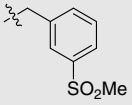	9.0 (n = 9)	>1100	0.35	Positive
1m	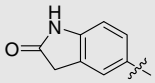	CF_3	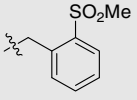	59	15	0.55	Positive
1n	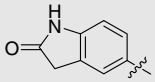	CF_3	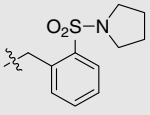	170 (n = 4)	17 (n = 4)	>0.93	Positive
1o	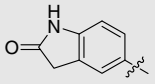	CF_3	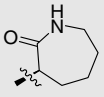	300	49	0.55	Positive
1p	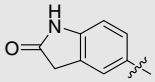	CF_3	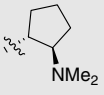	810, 1600	53	<0.26	Positive

(*continued on next page*)

Table 1 (*continued*)

Compound	X	Y	Z	FAK IC_{50}[a] (nM)	PYK2 IC_{50}[b] (nM)	HLM Eh[c]	RMA[d,e]
1q	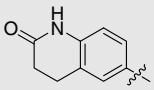	CF_3	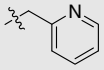	38	210	0.29	Positive
1r	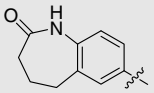	CF_3		N.T.	33	N.T.	Positive

[a] FAK ELISA protocol. IC_{50} values represent the concentration required to inhibit 50% of poly-Glu-Tyr phosphorylation by GST:FAK (see: Ref. 19). Numbers indicate IC_{50} values generated from individual 6-point concentration response relationships in triplicate.

[b] PYK2 ELISA protocol. IC_{50} values represent the concentration required to inhibit 50% of poly-Glu-Tyr phosphorylation by GST:PYK2 (see: Ref. 19). Numbers indicate IC_{50} values generated from individual 6-point concentration response relationships in triplicate.

[c] Eh = in vitro hepatic extraction ratio, which is obtained from dividing estimated hepatic blood clearance of test compounds by the human hepatic blood flow of 20 mL/min/kg. Protocols for measuring half-lives in HLM and subsequent scaling to blood clearance have been published (see: Ref. 20).

[d] For compound **1b**, the molecular mass of the GSH-EE conjugate corresponded to addition of the thiol to a *N*-demethylated metabolite of the parent compound.

[e] For all other analogs, the molecular mass of the GSH-EE conjugate corresponded to addition of the thiol to the parent compound suggesting a similar bioactivation mechanism as shown for **1a**.

[f] Buckbinder et al. (see: Ref. 3) reports an IC_{50} of 31 nM for compound **1a** using a fluorescence polarization assay.

The product ion spectrum obtained by collision-induced dissociation (CID) of the MH^+ at *m*/*z* 812 for the isomeric GSH conjugates of **1a** produced identical fragment ions at *m*/*z* 724, 683, 623, 551, 539, and 198 (Fig. 1, panel B). The presence of the fragment ion at *m*/*z* 198[13] established that the C4 substituent was unaltered (see Fig. 1, panel B), indicating that GSH conjugation had occurred on the 5-aminooxindole or the trifluoromethylpyrimidine ring. The fragment ion at *m*/*z* 683 corresponded with the loss of the pyroglutamate moiety, which represents a characteristic fragment ion derived from GSH conjugates.[14] The fragment ion at *m*/*z* 539 was assigned as a cleavage adjacent to the cysteinyl thioether moiety with charge retention on the **1a** residue. The occurrence of the fragment ion at *m*/*z* 539 is consistent with the presence of an aromatic thioether motif in **1a**.[14] A proposed structure for the GSH conjugate(s) of **1a** that is consistent with the observed mass spectrum, is shown in Figure 1, panel B. The assigned regiochemistry of GSH addition as shown is arbitrary and for illustrative purposes only. A mechanism for its formation is shown in Scheme 2. Thus, P450-catalyzed two-electron oxidation of the 5-aminooxindole motif would generate the electrophilic *bis*-imine followed by Michael addition of GSH. A similar mechanism has recently been reported for a series of aryl amide tyrosine kinase inhibitors.[15] In general, this bioactivation sequence is analogous to the one observed with the prototypic hepatotoxin and anti-inflammatory agent acetaminophen.[16] Not surprisingly, all analogs possessing the 5-aminooxindole group at C2 were positive in the reactive metabolite assessments (see Table 1). Likewise, analogs **1q** and **1r**, in which the oxindole group was replaced with the corresponding dihydroquinolinone and tetrahydrobenzazepinone functionalities, respectively, also formed sulfydryl conjugates (Table 1). The molecular masses of these conjugates suggested that a similar bioactivation pathway involving the *para*-aminophenylacetamido framework was operative.

Our strategy was to eliminate the bioactivation liability observed with **1a** while maintaining or improving PYK2 potency, FAK selectivity and HLM stability. The X-ray co-crystal structure of pyrimidine **1n** bound to the ATP binding pocket of PYK2 is detailed in Figure 2.[17] The structure shows N1 of the pyrimidine and the C2 amino group making key hydrogen bonds to the hinge residue (Tyr505). More importantly, the structure shows the 5-membered ring lactam of the oxindole partially solvent exposed. Thus, it was thought that making small structural modifications to the lactam ring should be possible without adversely affecting PYK2 activity. Furthermore, based on the propensity of electron-rich aryl rings to undergo bioactivation by CYP enzymes,[18] we reasoned that replacing the fused lactam, an electron donating moiety, in **1a** with an electron withdrawing group should lower the compound's susceptibility to undergo CYP-mediated bioactivation. For this exercise, we limited the C5 substituent to trifluoromethyl and the C4 substituent to either cyclopentanediamine or *N*-methyl-methanesulfonamidobenzylamine since it was unlikely that these groups contribute significantly to the bioactivation process.

Compounds possessing modifications to the C2 5-aminooxindole moiety are shown in Table 2. We were pleased to discover that analogs possessing a variety of aryl amines at C2 were negative in the RM assay. Furthermore, several of the compounds showed PYK2 activity and FAK selectivity similar to their corresponding 5-aminooxindole counterparts. Thus, isoindolinone **2a**, where the carbonyl and amino groups of the lactam ring of **1a** have been reversed, displayed similar PYK2 potency and FAK selectivity to that of **1a**. Tetrahydrobenzazepinone **2b** was negative in the RM assay, but it was 3-fold less potent against PYK2 and was less stable in HLM. Both dihydrobenzothiophene-*S*,*S*-dioxide **2c** and dihydrobenzisothiazole-*S*,*S*-dioxide **2d** showed similar PYK2 activity and HLM stability compared to the corresponding oxindole analog **1p**. In general, the 6,5-fused heterocycles, where an electron withdrawing group (EWG) is directly attached to the ring, were effective replacement groups for the oxindole. Analogs **2e**–**2i**, which possess a directly linked EWG but do not contain a fused ring, also eliminated the bioactivation potential. The PYK2 potency and HLM stability of these analogs was in-line with the corresponding fused ring compounds. Sulfone **2e** displayed good stability in HLM, whereas sulfonamide **2g** and carboxamides **2h** and **2i** were less stable than their fused ring counterparts.

Azanorbornene **2j** is an example of an analog that does not possess a directly linked EWG yet was negative in the RM assay. Interestingly, this analog was 9-fold more potent against PYK2 than the corresponding oxindole analog **1p**. It is possible the acetamide carbonyl on the azanorbornene is making a favorable interaction out of the plane of the benzene ring with PYK2, which would not be possible with the planar oxindole. Pyridine **2k** and imidazopyridine **2l** represent two additional examples that were negative in the RM assay yet do not possess a directly linked EWG. In these cases, it is likely the pyridine nitrogen has a significant effect on the electron density of the aryl ring such that a bioactivation mechanism similar to **1a** is not favored.

While it was reasonable to anticipate lack of GSH conjugates for compounds **2a**–**2l** due to disruption of the electron-rich *bis*-aniline architecture, we were surprised to find that benzosultam derivatives **2m** and **2n** were devoid of sulfydryl conjugate formation in the HTS reactive metabolite screen as well as in separate HLM incubations

Table 2
In vitro IC_{50} values for FAK and PYK2 inhibition, HLM stability and propensity for reactive metabolite formation by compounds **2a–2n**

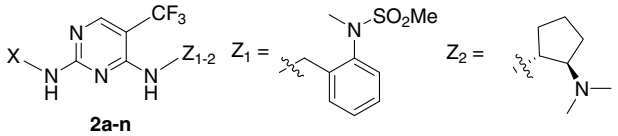

2a-n

Compound	X	Z	FAK IC_{50}[a] (nM)	PYK2 IC_{50}[b] (nM)	In vitro HLM Eh[c]	RMA[d]
2a	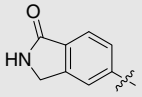	1	0.50	5.0	N.T.	Negative
2b	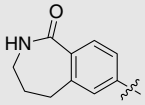	2	880	143	0.59	Negative
2c	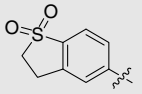	2	623	67 ($n = 3$)	0.37	Negative
2d	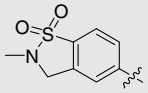	2	3200	25, 65	0.44	Negative
2e	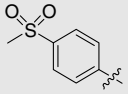	2	1300, 2000	95 ($n = 4$)	<0.28	Negative
2f	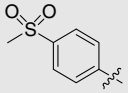	1	0.94	35, 66	0.93	Negative
2g	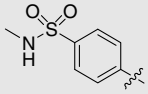	2	3800, 4500[e]	154[f]	0.66	Negative
2h	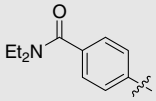	2	3300 ($n = 4$)[e]	72 ($n = 4$)[f]	0.66	Negative
2i	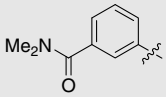	2	3900, 4000[e]	99h[f]	0.66	Negative
2j	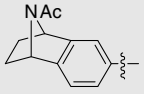	2	72	6	0.63	Negative
2k		2	4100, 6900[e]	430[f]	0.48	Negative
2l	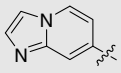	2	N.T.	150[f]	0.41	Negative
2m	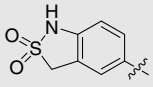	1	1.0, 5.0	2.0, 3.0	0.71	Negative

(*continued on next page*)

Table 2 (*continued*)

Compound	X	Z	FAK IC_{50}[a] (nM)	PYK2 IC_{50}[b] (nM)	In vitro HLM Eh[c]	RMA[d]
2n	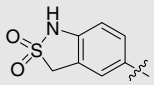	2	>650 (n = 5)	50 (n = 5)	<0.26	Negative

[a] FAK ELISA protocol. IC_{50} values represent the concentration required to inhibit 50% of poly-Glu-Tyr phosphorylation by GST:FAK (see: Ref. 19). Numbers indicate IC_{50} values generated from individual 6-point concentration response relationships in triplicate.

[b] PYK2 ELISA protocol. IC_{50} values represent the concentration required to inhibit 50% of poly-Glu-Tyr phosphorylation by GST:PYK2 (see: Ref. 19). Numbers indicate IC_{50} values generated from individual 6-point concentration response relationships in triplicate.

[c] Eh = hepatic extraction ratio, which is obtained from dividing estimated hepatic blood clearance of test compounds by the human hepatic blood flow of 20 mL/min/kg. Protocols for measuring half-lives in HLM and subsequent scaling to blood clearance have been published (see: Ref. 20).

[d] Reactive metabolite assessments in the HTS screening mode were conducted using GSH-EE as trapping agent in NADPH-supplemented HLM.

[e] FAK fluorescence polarization (FP) protocol as described in Ref. 3 using FAK kinase domain construct as described in Ref. 19 IC_{50} values represent the concentration to inhibit 50% of the phosphorylation of a peptide substrate relative to vehicle control. Numbers indicate IC_{50} values generated from individual 8-point concentration response relationships in triplicate.

[f] PYK2 fluorescence polarization (FP) protocol as described in Ref. 3 IC_{50} values represent the concentration to inhibit 50% of the phosphorylation of a peptide substrate relative to vehicle control. Numbers indicate IC_{50} values generated from individual 8-point concentration response relationships in triplicate.

with GSH. The precise reason(s) for lack of GSH conjugate formation, despite the presence of the *para*-aminophenylsulfonamido group, remains unclear and is the subject of an independent investigation in our laboratory. In addition to the lack of reactive metabolite liability, both benzosultams **2m** and **2n** show good PYK2 potency. Benzosultam **2n** was further attractive in that it showed 20-fold FAK selectivity and was stable in HLM.

In summary, we have described the synthesis and SAR for a series of diaminopyrimidines as PYK2 inhibitors. Using a combination of library and traditional medicinal chemistry techniques,

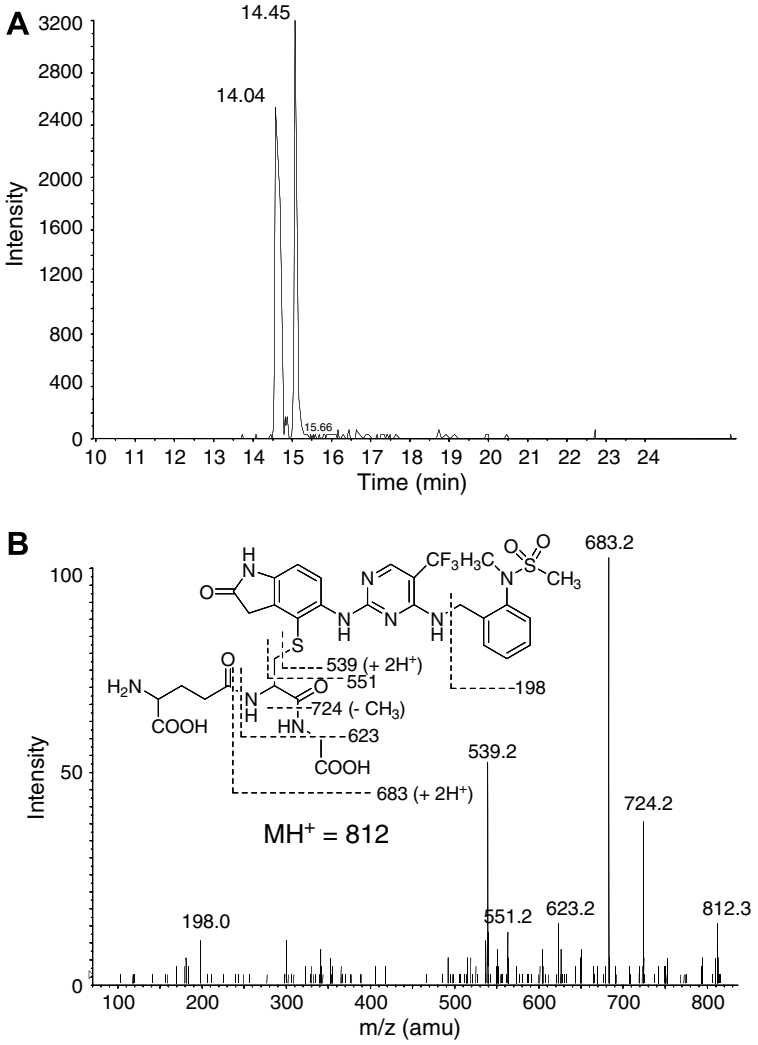

Figure 1. Extracted ion chromatogram (panel A) of an incubation mixture containing **1a** (10 μM) and NADPH- and GSH-supplemented HLM. Panel B indicates the CID spectrum of the MH^+ ion (m/z 812) of the GSH conjugate at retention time = 14.45 min. The origins of the characteristic ions are as indicated. Both GSH conjugates exhibited an identical mass spectrum suggesting that they were regioisomers. Assigned regiochemistry for GSH addition is arbitrary and for illustrative purposes only.

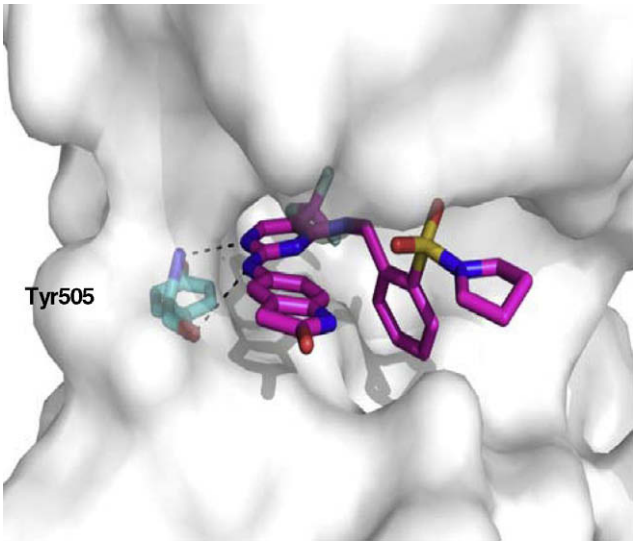

Figure 2. Crystal structure of compound **1n** (magenta) bound to PYK2. Dashed lines show hydrogen bond contacts to the hinge region.

we were able to transform a FAK-selective chemical series into compounds with good PYK2 potency and 10- to 20-fold selectivity against FAK. It was later determined that the vast majority of these compounds were positive in a HTS RM assay, indicating a potential toxicological liability for this set of compounds. The 5-aminooxindole moiety was identified as the likely culprit. Based on the proposed mechanism for bioactivation, as well as a combination of structure-based drug design and traditional medicinal chemistry techniques, we prepared a follow-up series of PYK2 inhibitors that were negative in the RM assay. Furthermore, many of these follow-up analogs and especially those possessing the C4 cyclopentanediamine, showed good PYK2 activity and FAK selectivity. Compounds **2c–2e, 2l**, and **2n** are further attractive in that they were stable in HLM.

Acknowledgments

We thank Jun Xiao, Kendra Nelson, Xumiao Zhao, and Samit Bhattacharya for the preparation of compounds **1q**, **2a**, and **2b**. We thank Donn Wishka, Joel Arcari, Jim Southers, and Artie Brosius for the preparation of compound **2j**. We thank Elizabeth Schnippel for the preparation of compounds **1b** and **1j**. We thank the ADME CoE group for in vitro HTS ADME data.

References and notes

1. Schlaepfer, D. D.; Hauck, C. R.; Sieg, D. J. *Prog. Biophys. Mol. Biol.* **1999**, *71*, 435.
2. (a) Guinamard, R.; Okigaki, M.; Schlessinger, J.; Ravetch, J. V. *Nat. Immunol.* **2000**, *1*, 36; (b) Okigaki, M.; Davis, C.; Falasca, M.; Harroch, S.; Felsenfeld, D. P.; Sheetz, M. P.; Schlessinger, J. *Proc. Natl. Acad. Sci. U.S.A.* **2003**, *100*, 10740.
3. Buckbinder, L.; Crawford, D. T.; Qi, H.; Ke, H.-Z.; Olson, L. M.; Long, K. R.; Bonnette, P. C.; Baumann, A. P.; Hambor, J. E.; Grasser, W. A.; Pan, L. C.; Owen, T. A.; Luzzio, M. J.; Hulford, C. A.; Gebhard, D. F.; Paralkar, V. M.; Simmons, H. A.; Kath, J. C.; Roberts, W. G.; Smock, S. L.; Guzman-Perez, A.; Brown, T. A.; Li, M. *Proc. Natl. Acad. Sci. U.S.A.* **2007**, *104*, 10619.
4. (a) Kalgutkar, A. S.; Gardner, I.; Obach, R. S.; Shaffer, C. L.; Callegari, E.; Henne, K. R.; Mutlib, A. E.; Dalvie, D. K.; Lee, J. S.; Nakai, Y.; O'Donnell, J. P.; Boer, J.; Harriman, S. P. *Curr. Drug Metab.* **2005**, *6*, 161; (b) Evans, D. C.; Watt, A. P.; Nicoll-Griffith, D. A.; Baillie, T. A. *Chem. Res. Toxicol.* **2004**, *17*, 3; (c) Ju, C.; Uetrecht, J. P. *Curr. Drug Metab.* **2002**, *3*, 367.
5. The addition of an aliphatic or aryl amine to 2,4-dichloro-5-trifluoromethylpyrimidine is typically nonselective. This is in contrast to many other 2,4-dichloro-5-substituted pyrimidines where the addition of an amine is typically selective for the 4-position. The conditions for *Method A* were specifically developed for the selective addition of amines to the 2-position of 2,4-dichloro-5-trifluoromethyl pyrimidine, see: Kath, J. C.; Richter, D. T.; Luzzio, M. J. US Patent 7,122,670, October 16, 2006.
6. Compound **2k** was prepared by a four step procedure according to the following scheme:

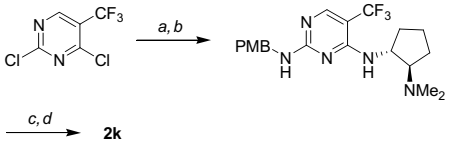

Reagents and conditions: (a) 2.0 equiv $ZnCl_2$ (1.0 M solution in ether), CH_2Cl_2–^{t}BuOH (1:1), −5 °C, 1 h; *para*-methoxybenzylamine, 1.1 equiv Et_3N, −5 °C → room temperature 16 h, 25%; (b) (1*R*,2*R*)-*N*,*N*-dimethylcyclopentane-1,2-diamine, Na_2CO_3, NMP, 80 °C, 2 h, 92%; (c) TFA–chloroform (5:1, 0.16 M), 50 °C, 16 h, 70%; (d) 4-bromopyridine, $Pd_2(dba)_3$ (0.02 equiv), Cs_2CO_3 (1.40 equiv), XANTPHOS (0.04 equiv), dioxane, 100 °C, 16 h, 52%.
7. Kath, J. C.; Luzzio, M. J. Patent Cooperation Treaty WO 2004/056807, July 08, 2004.
8. Avraham, H.; Park, S. Y.; Schinkmann, K.; Avraham, S. *Cell. Signal.* **2000**, *12*, 123.
9. Soglia, J. R.; Harriman, S. P.; Zhao, S.; Barberia, J.; Cole, M. J.; Boyd, J. G.; Contillo, L. G. *J. Pharm. Biomed. Anal.* **2004**, *36*, 105.
10. Kalgutkar, A. S.; Fate, G.; Didiuk, M. T.; Bauman, J. *Expert Rev. Clin. Pharmacol.* **2008**, *1*, 515.
11. Glutathione-ethyl ester (GSH-EE) was used as the exogenous trapping agent in the HTS reactive metabolite assay based on previous studies from our the laboratories that revealed the improved sensitivity in sulfydryl conjugate detection with ethyl ester derivative of GSH relative to the free carboxylic acid, a feature attractive for HTS assays (see Ref. 9).
12. Reactive metabolite assessment: HLM (P450 concentration = 0.3 μM) containing test compound (10 μM), GSH or GSH-EE (1 mM) and NADPH (1.2 mM) in 100 mM potassium phosphate buffer (pH 7.4) were incubated for 30 min at 37 °C. The final incubation volume was 250 μL. Samples without either NADPH or test compound were used as negative controls. The reactions were quenched by the addition of acetonitrile (375 μL) and after centrifugation (3000*g*, 15 min) the supernatant was concentrated under a steady nitrogen stream. Sulfydryl conjugates were extracted from each sample using solid phase extraction. A capillary liquid chromatography system (Dionex Corp., Sunnyvale, CA) was used for LC/MS/MS analysis. Chromatography was performed in a Vydac™ 300 μm id × 5 cm C18 column that contained 5 μm particles with a pore size of 300 Å (Grace Vydac, Hesperia, CA). Sulfydryl conjugates were chromatographed using a binary mobile phase consisting of acetonitrile:ammonium formate (5 mM):formic acid (10:90:0.05, v/v/v) (solvent A) and acetonitrile:ammonium formate (5 mM):formic acid (80:20:0.05, v/v/v) (solvent B) at a flow rate of 5 μL/min. A Thermo-Finnigan Quantum triple quadrupole mass spectrometer with an orthogonal electrospray ionization interface (Thermo-Finnigan Corp., San Jose, CA) was used in the analysis. Electrospray ionization was initiated by applying voltage of 3.8 kV (positive polarity). The auxiliary gas pressure and source transfer capillary temperature were maintained at 0 and 250 °C, respectively, throughout the study.
13. The fragment ion at *m*/*z* 198 was also observed in the CID spectrum of **1a**. Furthermore, metabolite identification study on **1a** in NADPH-supplemented human liver microsomes revealed the presence of the *N*-demethylated metabolite (*N*-demethylation of the C4 sulfonamide group, $MH^+ = 493$) with a base fragment ion at *m*/*z* 184 (corresponding to loss of 14 amu from the fragment ion at *m*/*z* 198).

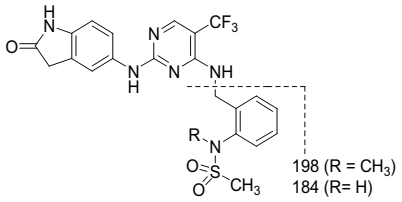

14. Baillie, T. A.; Davis, M. R. *Biol. Mass Spectrom.* **1993**, *22*, 319.
15. Meegala, S. K.; Wall, M. J.; Chen, J.; Wilson, K. J.; Ballentine, S. K.; DesJarlais, R. L.; Schubert, C.; Crysler, C. S.; Chen, Y.; Molloy, C. J.; Chaikin, M. A.; Manthey, C. L.; Player, M. R.; Tomczuk, B. E.; Illig, C. R. *Bioorg. Med. Chem. Lett.* **2008**, *18*, 3632.
16. Dahlin, D. C.; Miwa, G. T.; Lu, A. Y.; Nelson, S. D. *Proc. Natl. Acad. Sci. U.S.A.* **1984**, *81*, 1327.
17. The atomic coordinates for the X-ray structure of PYK2 in complex with compound **1n** have been deposited into the RCSB protein data bank: RCSB ID Code rcsb049736, and under PDB ID Code **3ET7**.
18. Koymans, L.; Donne-Op den Kelder, G. M.; te Koppele, J. M.; Vermeulen, N. P. *Xenobiotica* **1993**, *23*, 633.
19. Slack-Davis, J. K.; Martin, K. H.; Tighman, R. W.; Iwanicki, M.; Ung, E. J.; Autry, C.; Luzzio, M. J.; Cooper, B.; Kath, J. C.; Roberts, W. G.; Parsons, J. T. *J. Biol. Chem.* **2007**, *282*, 14845.
20. Obach, R. S. *Drug Metab. Dispos.* **1999**, *27*, 1350.